

# An independent test of the photometric selection of white dwarf candidates using LAMOST DR3

N. P. Gentile Fusillo<sup>1</sup>, A. Rebassa-Mansergas<sup>2</sup>, B.T. Gänsicke<sup>1</sup>, X.-W. Liu<sup>2,3</sup>, J.J. Ren<sup>3</sup>, D. Koester<sup>4</sup>, Y. Zhan<sup>5</sup>, Y. Hou<sup>5</sup>, Y. Wang<sup>5</sup>, M. Yang<sup>6</sup>

<sup>1</sup> *Department of Physics, University of Warwick, Coventry, CV4 7AL, UK*

<sup>2</sup> *Kavli Institute for Astronomy and Astrophysics, Peking University, 100871 Beijing, P. R. China*

<sup>3</sup> *Department of Astronomy, Peking University, Beijing 100871, P. R. China*

<sup>4</sup> *Institut für Theoretische Physik und Astrophysik, University of Kiel, 24098 Kiel, Germany*

<sup>5</sup> *Nanjing Institute of Astronomical Optics & Technology, National Astronomical Observatories, Chinese Academy of Sciences, Nanjing 210042, P. R. China*

<sup>6</sup> *Key Laboratory of Optical Astronomy, National Astronomical Observatories, Chinese Academy of Sciences, Beijing 100012, P. R. China*

17 June 2015

## ABSTRACT

In Gentile Fusillo et al. (2015) we developed a selection method for white dwarf candidates which makes use of photometry, colours and proper motions to calculate a *probability of being a white dwarf* ( $P_{\text{WD}}$ ). The application of our method to the Sloan Digital Sky Survey (SDSS) data release 10 resulted in  $\simeq 66,000$  photometrically selected objects with a derived  $P_{\text{WD}}$ , approximately  $\simeq 21000$  of which are high confidence white dwarf candidates. Here we present an independent test of our selection method based on a sample of spectroscopically confirmed white dwarfs from the LAMOST (Large Sky Area Multi-Fiber Spectroscopic Telescope) survey. We do this by cross matching all our  $\simeq 66,000$  SDSS photometric white dwarf candidates with the over 4 million spectra available in the third data release of LAMOST. This results in 1673 white dwarf candidates with no previous SDSS spectroscopy, but with available LAMOST spectra. Among these objects we identify 309 genuine white dwarfs. We find that our  $P_{\text{WD}}$  can efficiently discriminate between confirmed LAMOST white dwarfs and contaminants. Our white dwarf candidate selection method can be applied to any multi-band photometric survey and in this work we conclusively confirm its reliability in selecting white dwarfs without recourse to spectroscopy. We also discuss the spectroscopic completeness of white dwarfs in LAMOST, as well as deriving effective temperatures, surface gravities and masses for the hydrogen-rich atmosphere white dwarfs in the newly identified LAMOST sample.

**Key words:** (stars:) white dwarfs - surveys - catalogues

## 1 INTRODUCTION

Main sequence stars of masses  $M \lesssim 8 - 10.5 M_{\odot}$  are destined to become white dwarfs (Iben et al. 1997, Smartt et al. 2009). White dwarfs are therefore the most common stellar remnants in the Galaxy. However, because of their small radii, and hence low luminosities, constructing a large, homogeneous and unbiased sample of white dwarfs is still an ongoing challenge.

The advent of modern large scale observational surveys has allowed to constrain fundamental parameters such as the white dwarf space density (Limoges & Bergeron 2010; Sion et al. 2014), mass distribution and mass function (Bergeron et al. 1992;

Liebert et al. 2005; Kepler et al. 2007; Falcon et al. 2010; Tremblay et al. 2013; Kleinman et al. 2013), luminosity function (Oswalt et al. 1996; De Gennaro et al. 2008; Torres et al. 2014; Cojocaru et al. 2014) and formation rate (Hu et al. 2007; Verbeek et al. 2013). However, the white dwarf samples used in these studies are inevitably affected by selection effects, and it is difficult to quantify how and to what extent the observational biases affect the derived results. We recently developed a selection method which enables us to identify high-confidence white dwarf candidates in large multi-colour photometric surveys. The application of our method to SDSS data release (DR) 10 allowed us to investigate the spectroscopic biases of SDSS DR10 and resulted in a catalogue of 65,768 bright ( $g \leq 19$ )

point sources (Gentile Fusillo et al. 2015) with computed *probability of being a white dwarf* ( $P_{WD}$ ). Using our catalogue it is possible to select  $\sim 14,000$  high-confidence white dwarf candidates that have not yet received any spectroscopic follow up, which is ultimately needed to measure their fundamental parameters such as mass and cooling age. Spectroscopic follow-up will also help in identifying rare white dwarf types, which are key objects for a wide variety of studies such as exploring the late evolutionary stages of a wide range of progenitor stars (Schmidt et al. 1999; Dufour et al. 2010; Gänsicke et al. 2010), searching for low-mass companions (Farihi et al. 2005; Girven et al. 2011; Steele et al. 2013), metal polluted white dwarfs (Sion et al. 1990; Zuckerman & Reid 1998; Dufour et al. 2007; Koester et al. 2014) and white dwarfs with dusty or gaseous planetary debris discs (Gänsicke et al. 2006; Farihi et al. 2009; Debes et al. 2011; Wilson et al. 2014).

The recently initiated Large Sky Area Multi-Object Fiber Spectroscopic Telescope (LAMOST; Luo et al. 2015) survey provides hundreds of thousand of spectra per year and its sky coverage overlaps to a large degree with the photometric footprint of SDSS (Fig 1). In this work we cross-match our catalogue of photometric SDSS white dwarf candidates with the over 4 million spectra obtained to date by LAMOST and find spectroscopy spectra for 309 white dwarfs. We use this new set of white dwarfs to test our photometric selection method, as well as to analyse the effects of the target selection algorithm of LAMOST on the observed white dwarf population. We also provide the stellar parameters of the newly-identified DA (hydrogen dominated atmosphere) white dwarfs, namely the effective temperatures, surface gravities and masses.

## 2 THE LAMOST SURVEY

LAMOST is a quasi-meridian reflecting Schmidt telescope of effective aperture  $\sim 4\text{m}$  located at Xinglong Observing Station in the Hebei province of China (Cui et al. 2012). LAMOST uses 16 fiber-fed spectrographs each equipped with a red and a blue channel CDD camera. Each spectrograph counts with 250 fibers, thus LAMOST is able to obtain a total of 4,000 simultaneous spectra. The wavelength coverage of the spectra is  $\sim 3800\text{--}9000\text{ \AA}$  at a resolving power of  $\sim 1,800$ . Although the flux calibration of the LAMOST spectra is relative (Song et al. 2012), the spectral energy distribution is correctly characterized and classifications based on visual inspection of the spectra can be considered as reliable.

LAMOST started operation in 2009 and began a five-year regular survey in 2012. This survey consists of two main parts with different science goals and target selection criteria (Zhao et al. 2012). The LAMOST Extra-Galactic Survey (LEGAS) studies the large scale structure of the Universe. The LAMOST Experiment for Galactic Understanding and Exploration (LEGUE) focuses on characterizing the structure and evolution of the Milky Way (Deng et al. 2012) and is sub-divided into three sub-surveys (Carlin et al. 2012; Chen et al. 2012; Liu et al. 2014; Yuan et al. 2015): the spheroid, the disk, and the Galactic anti-center.

The current number of available LAMOST spectra is  $\sim 4.6$  million. These include the full second data release

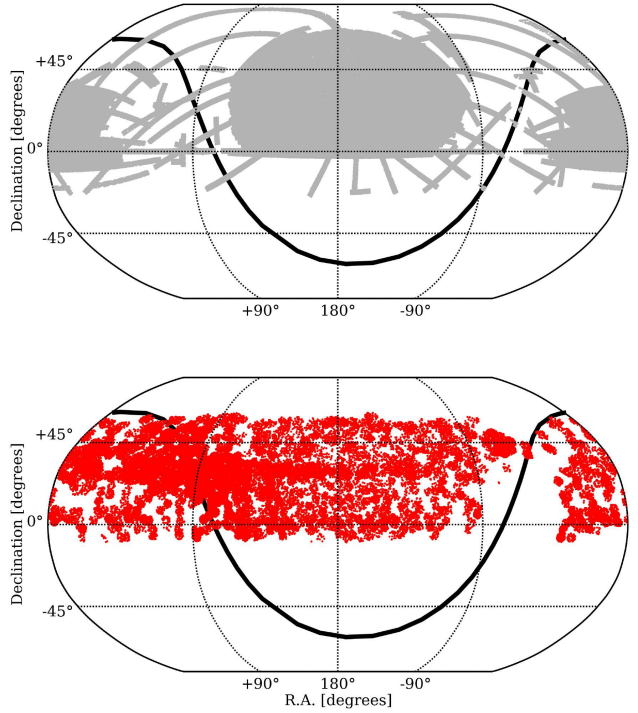


**Figure 1.** Photometric coverage of SDSS DR10 (top panel) and LAMOST DR3 pointings (bottom panel). The black line indicates the location of the Galactic plane.

(DR2) plus the first three months of data of the third data release (DR3).

## 3 SDSS PHOTOMETRIC WHITE DWARF CANDIDATES OBSERVED BY LAMOST

The catalogue of Gentile Fusillo et al. (2015) includes 65,768 bright ( $g \leq 19$ ) point sources selected according to their available SDSS photometry and colours. The catalogue contains not only white dwarfs, but also quasars and other blue stars, however each object has an associated  $P_{WD}$  calculated from its  $g - z$  colour and reduced proper motion.

We estimate that our catalogue contains  $\sim 14,000$  white dwarfs which have not yet received spectroscopic follow up in the latest data release of SDSS (DR12). The vast number of available LAMOST spectra, combined with the large overlap in the SDSS and LAMOST footprints (Fig. 1), implies that a considerable number of white dwarf candidates have most likely been observed by LAMOST. Consequently combining our catalogue of SDSS white dwarfs candidates with all available LAMOST spectra is not only a quick and reliable way to identify new white dwarfs, but also provides a further test to corroborate the reliability of our selection method.

We cross-matched all 65,768 objects from the Gentile Fusillo et al. (2015) catalogue with the list of the 4.6 million LAMOST spectra and retrieved 6,101 spectra corresponding to 5173 unique objects (Table 1). 3500 of these have also received SDSS spectroscopic follow up and 64 further objects had already been identified on the base of their LAMOST spectra as white dwarfs or white dwarf binaries

**Table 1.** Summary of the cross-matching of SDSS white dwarf candidates with LAMOST DR3

	n. of objects	n. of spectra
All objects from cross-match	5173	6101
SDSS and LAMOST spectra	3500	3964
of which WDs	774	1177
LAMOST spectra only	1673	2137
of which WDs	309	387
already published	64	97
unpublished	245	290

**Table 2.** Classification of the 2,040 unpublished LAMOST spectra of 1,609 white dwarf candidates from the Gentile Fusillo et al. (2015) catalogue.

Class	n. of objects	n. of spectra
DA	196	222
DB	5	6
DAB/DBA	2	2
DO	3	5
DC	10	12
DZ	3	3
Magnetic WD	2	2
WD+MS	4	4
CV	19	33
Planetary nebula	1	1
NLHS	393	538
QSO	546	678
K/M stars	3	3
Unreliable	422	531

by Zhang et al. (2013); Zhao et al. (2013); Ren et al. (2014); Rebassa-Mansergas et al. (2015).

Since the main goal of this project is to test our photometric selection method using an independent spectroscopic sample of white dwarfs, we limited ourselves to objects which have no SDSS spectroscopic counterpart. This reduced the sample to 2,040 spectra corresponding to 1,609 unique LAMOST objects; plus the 64 known LAMOST white dwarfs mentioned above. **Finally we visually classified all remaining white dwarf candidates with unpublished LAMOST spectra.** We subdivided the identified white dwarfs into 10 types (Table 2, Fig. 2), and the contaminants into 3 types: “K/M stars”, “Quasars” (QSOs) and “Narrow Line Hydrogen Stars” (NLHS), in which we group different stars with low-gravity hydrogen dominated atmospheres such as subdwarfs, extreme horizontal branch stars and A/B type stars. We also marked as “unreliable” all spectra which had a signal-to-noise ratio too low for a reliable classification. The results of our classification are summarized in Table 2.

Inspection of the Table reveals that we have identified 245 white dwarfs (with a total of 290 spectra), of which over 80 per cent have hydrogen dominated atmospheres (DA). DAs are known to constitute the vast majority of all white dwarfs (McCook & Sion 1999), so the ratio above is unsurprising. Querying the SIMBAD astronomical database, we

**Table 3.** LAMOST objects identified as previously unknown CVs.

Name	CRDR2 lightcurve
J003005.80+261726.3	yes
J010903.02+275010.0	yes
J013317.01+305329.8	yes
J013855.86+242939.2	yes
J052602.79+285121.3	no
J062402.64+270410.2	no
J074037.68+254109.4	yes
J171630.84+444124.5	yes
J172308.28+392455.2	yes

find that 57 of our 245 white dwarfs had already been identified as such (as single stars or part of binary systems) in other studies. In conclusion we report the discovery of 188 new white dwarfs.

### 3.1 Cataclysmic variables in the LAMOST sample

During the classification of LAMOST spectra we identified 19 cataclysmic variables (CV, Table 2). 10 of these objects are known CVs while the remaining nine are new discoveries. Considering the limited size of our white dwarf sample the number of CVs found is remarkably high. However, we are not aware of any aspects of the targeting strategy of LAMOST which could have led to preferential observation of CVs. A possible cause of this bias towards CVs may be that the strong emission features which characterize CVs can be easily recognized even in very noisy spectra. Indeed we find that most of the inspected LAMOST spectra of CVs are of low quality. In order to verify our classification of these objects we cross-matched our nine new CVs with the second data release of the Catalina survey (CSDR2, Drake et al. 2009). CSDR2 provides multi-epoch photometry for over 500 million objects and has been an extremely useful resource for various campaign which searched for CVs (e.g. Breedt et al. 2014, Drake et al. 2014). Two of our new CVs are not within the CSDR2 sky footprint, but we were able to recover and inspected Catalina light curves for the remaining seven (Table 3). A complete analysis of these light curves is beyond the scope of this article, but we conclude these objects indeed show variability compatible with that of a CV.

## 4 AN INDEPENDENT TEST OF THE GENTILE FUSILLO ET AL. 2015 WHITE DWARF SELECTION METHOD

In Gentile Fusillo et al. (2015) we tested the reliability of our white dwarf candidate selection method using a sample of 6,706 spectroscopically confirmed white dwarfs and over 20,000 contaminants with available SDSS spectra. For a given  $P_{WD}$  threshold, we defined *completeness* as the ratio of the number of white dwarfs in the spectroscopic sample with at least that associated probability to the total number of white dwarfs in the sample. Similarly *efficiency* was defined as the ratio of the number of white dwarfs selected by the probability cut to the number of all the ob-

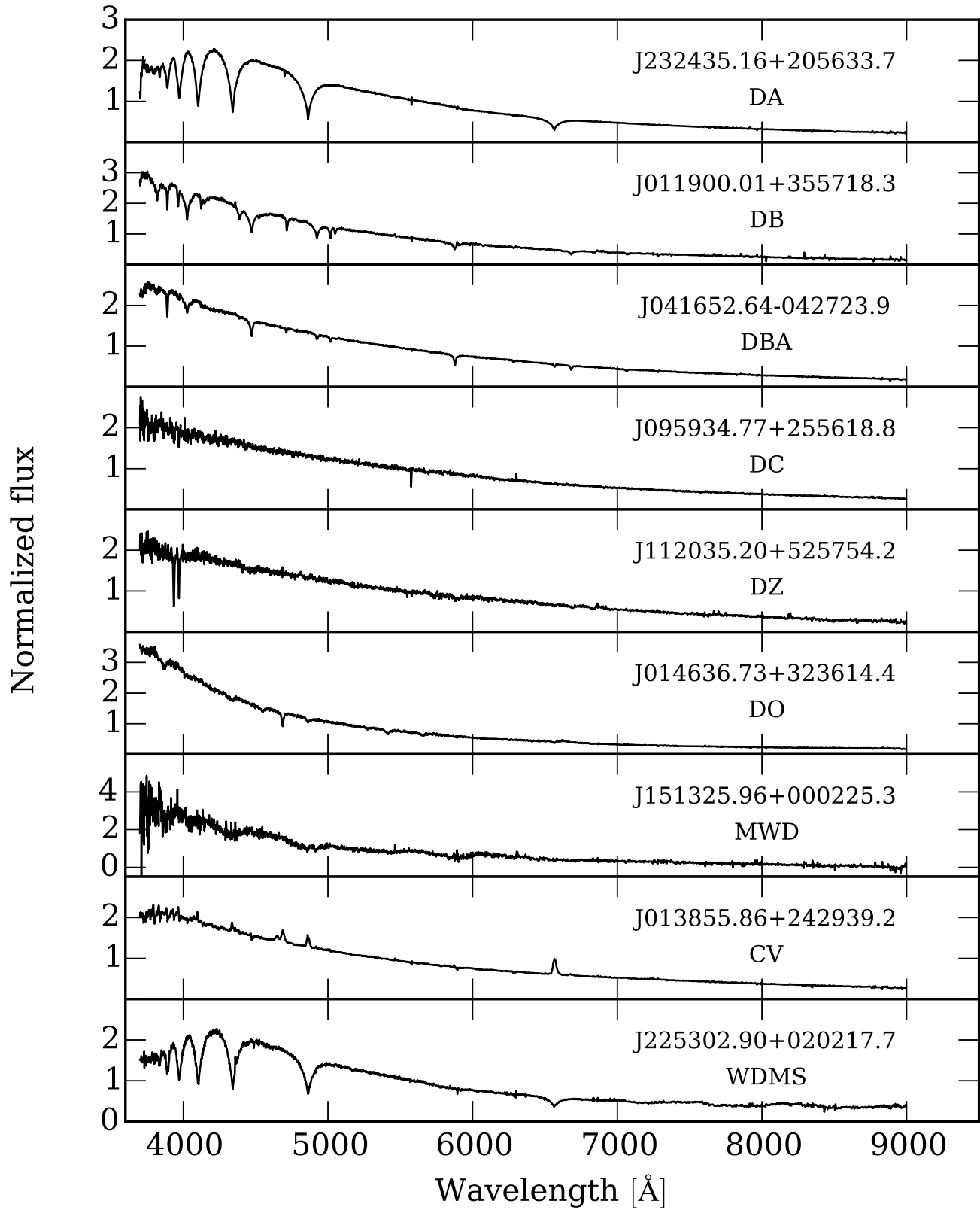


**Figure 2.** Sample LAMOST spectra of different types of white dwarfs

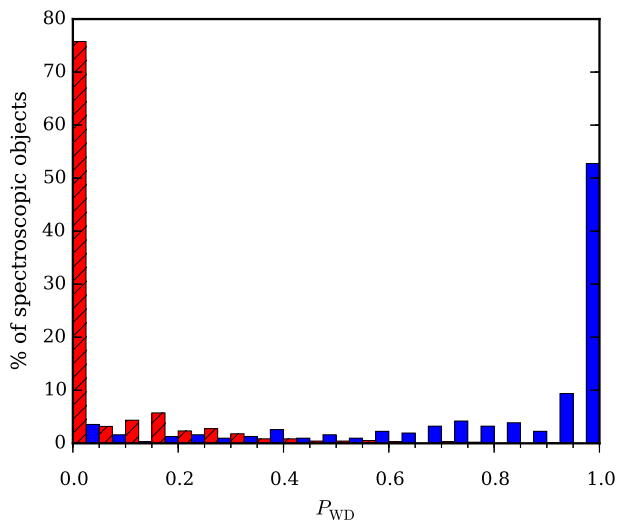


**Figure 3.** Distribution of all spectroscopically confirmed LAMOST white dwarfs (blue) and contaminants (red, shaded) as a function of  $P_{WD}$ .

jects retrieved by such selection. We concluded that our  $P_{WD}$  can be reliably used to discern between white dwarfs and contaminants. For example, selecting all objects with a  $P_{WD} \geq 0.41$  resulted in a sample of white dwarf candidates which is 95 per cent complete and 89.7 per cent efficient. One of the main strengths of the selection method of Gentile Fusillo et al. (2015) is that, even though it was developed using SDSS, it can in principle be applied to any large area survey which provides multi band photometry (e.g. VST ATLAS, APASS, SkyMapper, Pan-Starrs). The possibility of applying the selection method to surveys other than SDSS, however, stresses the need to test the robustness of our  $P_{WD}$  values on a sample of spectroscopically confirmed white dwarfs completely independent from SDSS. Even though our sample of 309 (64 known ones and 245 identified as part of this work) confirmed LAMOST white dwarfs and 876 contaminants is small compared to the SDSS spectroscopic sample, it provides a welcome opportunity to verify the reliability of our  $P_{WD}$  values. Figure 3 clearly shows that over  $\sim 80$  per cent of all LAMOST contaminants have  $P_{WD} < 0.2$  and virtually no contaminant has  $P_{WD} > 0.5$ . Similarly, the vast majority of LAMOST white dwarfs have  $P_{WD} > 0.5$ . Further inspection of Figure 3 reveals also that  $\sim 10$  per cent of the LAMOST white dwarfs have  $P_{WD} < 0.4$  and would be missed by the most reasonable selections based on  $P_{WD}$ , i.e. a probability cut at  $P_{WD} \geq 0.41$ . Inspection of these low probability objects reveals that the vast majority of these are CVs (see Sect 3.1). CVs have peculiar colours distinct from those of most single white dwarfs and the selection method of Gentile Fusillo et al. (2015) is not optimized for them. Nonetheless the statistic we compute on our LAMOST white dwarfs sample confirms the reliability of our selection method. The  $P_{WD}$  can confidently be used to select different samples white dwarfs according to the specific work one intends to carry out.

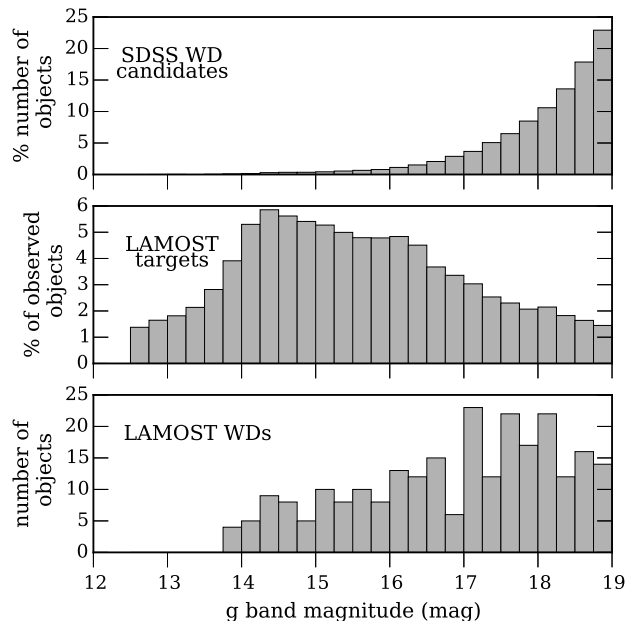


**Figure 5.** *Top panel:*  $g$ -band magnitude distribution of all SDSS white dwarf candidates from Gentile Fusillo et al. (2015). *Middle panel:*  $g$ -band magnitude distribution of a random sub-set of 100,000 objects with LAMOST spectroscopy. *Bottom panel:*  $g$ -band magnitude distribution of the newly identified LAMOST white dwarfs.

## 5 SPECTROSCOPIC COMPLETENESS OF THE WHITE DWARFS IDENTIFIED BY LAMOST

In Gentile Fusillo et al. (2015) we find that, to date, the SDSS white dwarf spectroscopic sample is  $\sim 40$  per cent complete. However, this number is averaged over the entire SDSS photometric footprint, large areas of which have not yet received any spectroscopic follow up. Furthermore, as we show in Fig. 4 (left panel), the spectroscopic completeness of SDSS white dwarfs is also very colour-dependent. For example, the spectroscopic completeness is highest for relatively cool white dwarfs with colours similar to those of quasars, a simple consequence of the target selection algorithm of SDSS. The LAMOST observing strategy differs from SDSS's both in terms of area of sky covered and target selection. Even though white dwarfs are only serendipitous or secondary targets for both surveys, the resulting spectroscopic samples are, to a certain degree, complementary. Figure 4 (right panel) illustrates that the spectroscopic completeness of LAMOST over the SDSS footprint does not dramatically depend on colour, although it does rise slightly in quasar-dominated areas. Naturally the number of white dwarfs increases at higher magnitudes as a larger volume is observed. However LAMOST observed mostly bright objects ( $g \simeq 14 - 16$ , Fig. 5) and therefore did not target the vast majority of photometrically selected white dwarfs. Consequently, even though the LAMOST white dwarf sample is less biased by colour it is limited in size, and the overall white dwarfs spectroscopic completeness is much lower than the SDSS one.

In order to compute the white dwarfs spectroscopic completeness of LAMOST we used the entire sample of

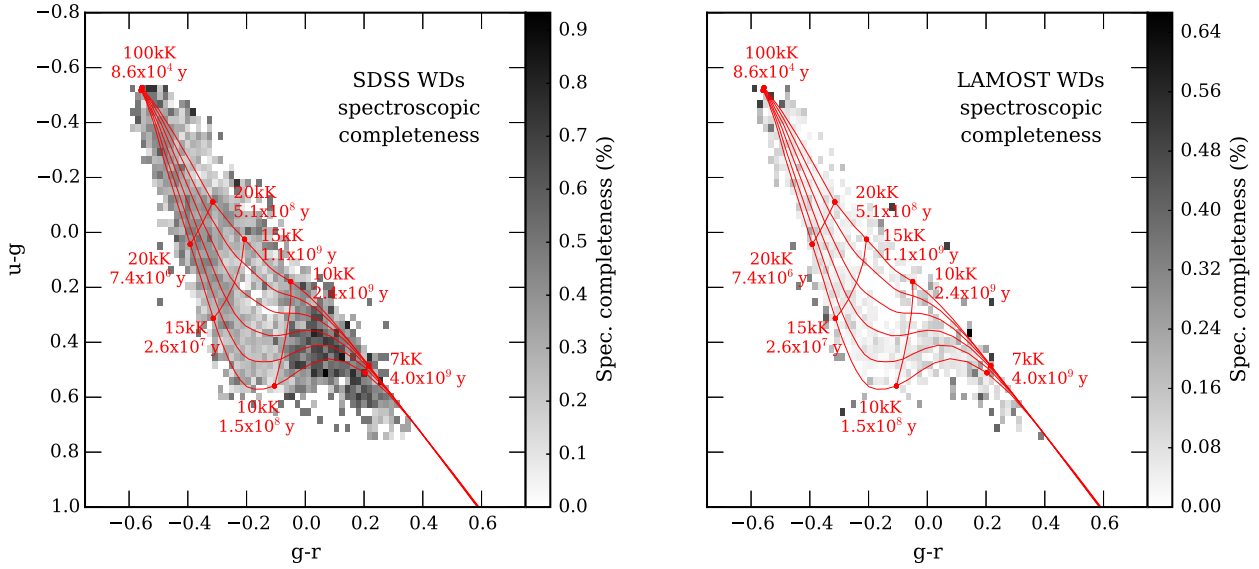


**Figure 4.** Spectroscopic completeness of SDSS white dwarfs (left panel) and LAMOST white dwarfs over the SDSS footprint (right panel). The values were computed as the ratio of spectroscopically confirmed white dwarfs to all high-confidence white dwarf candidates ( $P_{WD} \geq 0.41$ ) within the  $(u-g, g-r)$  colour-colour selection used in Gentile Fusillo et al. (2015). To correctly compute the spectroscopic completeness of LAMOST over the SDSS footprint, we used the entire sample of 1083 white dwarfs resulting from our initial cross match of LAMOST targets with the catalogue of Gentile Fusillo et al. (2015) (newly identified LAMOST WDs + already published LAMOST WDs + LAMOST WDs with SDSS spectra). White dwarf cooling tracks from Holberg & Bergeron (2006) are shown as overlay (red solid lines). The left panel clearly shows an area of higher spectroscopic completeness caused by the SDSS target selection algorithm, which favours the observations of QSOs (see sect.5).

1083 white dwarfs resulting from our initial cross match of LAMOST targets with the catalogue of Gentile Fusillo et al. (2015) (newly identified LAMOST WDs + already published LAMOST WDs + LAMOST WDs with SDSS spectra). However it is important to keep in mind that the final sample of new white dwarfs presented is not representative of all the white dwarfs observed by LAMOST. The catalogue of white dwarf candidates of Gentile Fusillo et al. (2015) can only be considered complete white dwarfs **with available proper motions**,  $T_{\text{eff}} \gtrsim 8000 \text{ K}$  and  $g \leq 19$ . Consequently the LAMOST white dwarf sample discussed here is affected by these same limitations. Even though cool white dwarf are particularly faint and LAMOST mostly targeted bright objects ( $g \simeq 14 - 16$ ), we expect that among the 4.6 million spectra collected to date there should be some cooler nearby white dwarfs which were not included in this work. Finally, LAMOST has also extensively covered areas of the sky which lie outside the SDSS footprint (e.g. the Galactic anti-center; Yuan et al. 2015) and any white dwarf observed in those areas would, by definition, not be included in the catalogue presented here.

## 6 STELLAR PARAMETERS

In this section we derive the stellar parameters of the newly identified LAMOST DA white dwarfs (Table 2). We do this following the fitting routine developed by Rebassa-Mansergas et al. (2007, 2010) adapted to LAMOST spectra (Rebassa-Mansergas et al. 2015). A brief description of this procedure is given here, and we refer the reader to the references above for further details.

To determine the effective temperature ( $T_{\text{eff}}$ ) and surface gravity ( $\log g [\text{g cm s}^{-2}]$ ) we fit the normalised  $\text{H}\beta$  to  $\text{He}$  line profiles of each spectrum with the DA model grid of Koester (2010) using a mixing-length parameter ( $\text{ML2}/\alpha$ ) of 0.6. Since the equivalent widths of the Balmer lines go through a maximum near  $T_{\text{eff}} = 13,000 \text{ K}$ , the line fitting provides two possible solutions, i.e. “hot” and “cold” solutions. We break this degeneracy fitting the entire white dwarf spectrum (continuum plus lines). The continuum spectrum of a DA WD is mostly sensitive to  $T_{\text{eff}}$ , therefore the best-fit value from the entire spectrum generally indicates which of the two solutions is the most reliable one. However, because of uncertainties in the LAMOST flux calibration (Section 2), the best-fit to the entire spectrum may be subject to systematic uncertainties. Thus, the choice between hot and cold solution is further guided by comparing the ultraviolet GALEX (Galaxy Evolution Explorer; Martin et al. 2005; Morrissey et al. 2005) and optical SDSS photometry to the fluxes predicted from each solution (where the SDSS fluxes are derived directly from the SDSS  $u, g, r, i, z$  magnitudes). Spectroscopic fits that use 1D atmosphere spectra models are known to systematically overestimate surface gravities for cool ( $\lesssim 12,000 \text{ K}$ ) white dwarfs (Koester et al. 2009; Tremblay et al. 2011). To overcome this effect we applied the 3D corrections of Tremblay et al. (2013) to  $T_{\text{eff}}$  and  $\log g$  determined above. Finally we obtained the masses of our white dwarfs by interpolating the obtained  $T_{\text{eff}}$  and  $\log g$  values with the tables of Renedo et al. (2010).

The  $T_{\text{eff}}$ ,  $\log g$  and masses we have determined are provided in the online catalogue which accompanies this article (Table 4). Inspection of the table reveals that these values



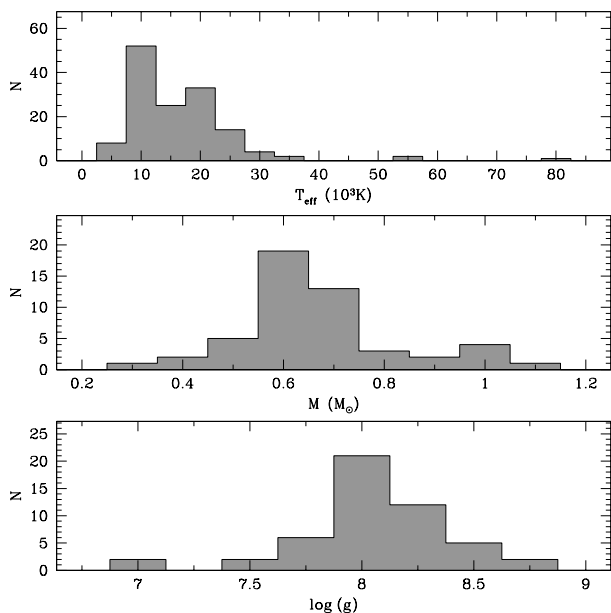


**Figure 6.** From top to bottom: effective temperature, mass and surface gravity distributions of the new LAMOST DA white dwarfs identified in this work.

are subject to large uncertainties in many cases. This is due to the low signal-to-noise ratio of many of the LAMOST spectra. In Figure 6 we show the  $T_{\text{eff}}$  distribution for DA white dwarfs with relative errors  $\leq 10$  per cent and the mass and  $\log g$  distributions for DA white dwarfs with errors in mass  $< 0.075 M_{\odot}$ . This results in 49 and 154 white dwarfs in the  $\log g$  and  $T_{\text{eff}}$  histograms respectively.

The mass distribution displays a broad and clear peak at  $0.6\text{--}0.7 M_{\odot}$ , as typically found in many previous studies (e.g. Liebert et al. 2005; Kleinman et al. 2013; Kepler et al. 2015). It also reveals the existence of both low-mass ( $\lesssim 0.5 M_{\odot}$ ) white dwarfs that may harbour unseen companions (Rebassa-Mansergas et al. 2011; Kilic et al. 2012) and high-mass ( $\gtrsim 0.8 M_{\odot}$ ) white dwarfs, some of which may be the result of mergers (Giammichele et al. 2012; Rebassa-Mansergas et al. 2015).

The  $T_{\text{eff}}$  distribution shows that our newly identified white dwarfs have generally  $10,000\text{--}20,000$  K, similar to the distribution obtained from SDSS spectroscopically selected white dwarfs (Kepler et al. 2015).

### 6.1 Comparison with stellar parameters from SDSS spectra

As mentioned in Section 3, 3500 objects from our initial sample have both SDSS and LAMOST spectra and 774 of them are white dwarfs (Table 1). This sample of objects provides a useful opportunity to compare DA white dwarf the stellar parameter obtained from LAMOST spectra with those obtained from SDSS spectra. In this comparison we decided to limit ourselves to DA white dwarfs with LAMOST spectra with a signal-to-noise ratio  $> 10$ . Applying these criteria results in a sample of 108 white dwarfs. We derive  $T_{\text{eff}}$  and  $\log g$  from both the SDSS spectra and the LAMOST spectra following the same procedure described in Section 6. Fig-

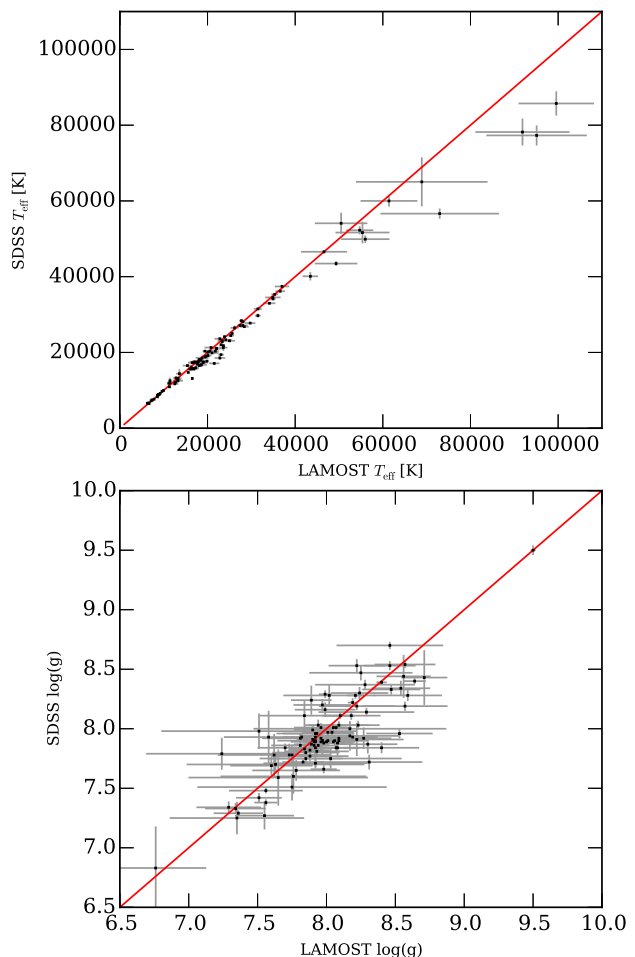


**Figure 7.** Comparison of stellar parameters (top:  $T_{\text{eff}}$ , bottom:  $\log g$ ) obtained by fitting the available SDSS and LAMOST spectra of 108 DA white dwarfs. Only objects which had a LAMOST spectrum with  $S/N > 10$  were used. The red lines reflect a simple 1:1 relationship.

ure 7 shows that the uncertainties in the LAMOST stellar parameters are generally significantly larger than the SDSS ones, this is caused by systematically lower signal-to-noise ratio of the LAMOST spectra. In order quantify the discrepancy between LAMOST and SDSS  $T_{\text{eff}}$  and  $\log g$  we define a quantity  $\tau$ :

$$\tau = \frac{\text{SDSS value} - \text{LAMOST value}}{\sqrt{\text{SDSS } \sigma^2 + \text{LAMOST } \sigma^2}} \quad (1)$$

We find that in 11 per cent of the cases the LAMOST  $T_{\text{eff}}$  values are overestimated by more than  $2\tau$  compared to the SDSS ones. When comparing the  $\log g$  values only 5.6 per cent of the objects show a comparable disagreement ( $\tau > 2$ ). We can conclude that the stellar parameters computed using SDSS and LAMOST spectra are broadly in agreement.

## 7 SUMMARY AND CONCLUSIONS

By cross matching all photometrically selected SDSS white dwarf candidates from the Gentile Fusillo et al. (2015) catalogue with the over 4 million spectra currently provided

by the LAMOST DR3 we identified 309, bright ( $g \leq 19$ ) white dwarfs with available LAMOST spectra of which only 64 were previously published as LAMOST white dwarfs. We inspected and classified the remaining 245 objects according to their spectral type and obtained  $T_{\text{eff}}$ ,  $\log g$  and masses for the DAs (which make up 80 per cent of the sample). We also find that 188 of these white dwarfs were previously unknown and are therefore new discoveries. Since LAMOST targeted mainly object with  $g \simeq 14 - 16$ , the sample of LAMOST white dwarfs presented here is limited in size. However, because SDSS and LAMOST follow different targeting strategies, the sample of LAMOST white dwarfs is not affected by the known and heavy biases of the SDSS white dwarf spectroscopic sample and constitute therefore a valuable complementary addition.

We also inspected the LAMOST available spectra of 864 additional SDSS photometric sources from the Gentile Fusillo et al. (2015) list and classified them as non-white dwarfs, i.e. contaminant objects. We used the spectroscopic samples of newly confirmed white dwarfs and contaminants to test the reliability of the Gentile Fusillo et al. (2015) selection method. Even with the relatively small size of our LAMOST spectroscopic sample we were able to verify that the Gentile Fusillo et al. (2015) *probabilities of being a white dwarf* can be reliably used to select samples of white dwarfs with completeness and efficiency close to 90 per cent. These results show that similar searches to the one presented here may be repeated in the near future (e.g with the forthcoming new data release of LAMOST) in a much more efficient way by relying more on the values of  $P_{\text{WD}}$  and therefore drastically reducing the amount of data to inspect by eye. Since the Gentile Fusillo et al. (2015) selection method can be applied to any multi-band photometric survey, future searches may also not be limited to the SDSS footprint.

The Gentile Fusillo et al. (2015) catalogue only includes SDSS white dwarf candidates with  $g \leq 19$ ,  $T_{\text{eff}} \gtrsim 8000\text{K}$  and reliable proper motions. Furthermore, LAMOST specifically targeted areas of the sky (e.g the Galactic anti-center) which were instead avoided by SDSS. Hence, the catalogue of new LAMOST white dwarfs presented here is not complete and should be considered as complementary to the work done in Gentile Fusillo et al. (2015), as well as a contribution to the total sample of known spectroscopic white dwarfs.

In the near future further multi-band photometry of LAMOST targets will become available thanks to the Panoramic Survey Telescope & Rapid Response System (Pan-STARRS, Morgan et al. 2014). The selection method for white dwarf candidates of Gentile Fusillo et al. (2015) could be applied to the Pan-STARRS database. Such application will lead to a new search for LAMOST white dwarfs outside the SDSS footprint.

## ACKNOWLEDGEMENTS

NPGF acknowledges the support of Science and Technology Facilities Council (STFC) studentships.

ARM acknowledges financial support from the Postdoctoral Science Foundation of China (grants 2013M530470 and 2014T70010) and from the Research Fund for International

Young Scientists by the National Natural Science Foundation of China (grant 11350110496).

The research leading to these results has received funding from the European Research Council under the European Unions Seventh Framework Programme (FP/2007-2013) / ERC Grant Agreement n. 320964 (WDTracer).

Guoshoujing Telescope (the Large Sky Area Multi-Object Fiber Spectroscopic Telescope, LAMOST) is a National Major Scientific Project which is built by the Chinese Academy of Sciences, funded by the National Development and Reform Commission, and operated and managed by the National Astronomical Observatories, Chinese Academy of Sciences.

**We thank the anonymous referee for his quick and constructive review.**

Funding for SDSS-III has been provided by the Alfred P. Sloan Foundation, the Participating Institutions, the National Science Foundation, and the U.S. Department of Energy Office of Science. The SDSS-III web site is <http://www.sdss3.org/>.

This research has made use of the SIMBAD database, operated at CDS, Strasbourg, France.

The CSS survey is funded by the National Aeronautics and Space Administration under Grant No. NNG05GF22G issued through the Science Mission Directorate Near-Earth Objects Observations Program. The CRTS survey is supported by the U.S. National Science Foundation under grants AST-0909182 and AST-1313422.

## REFERENCES

- Bergeron, P., Saffer, R. A., Liebert, J., 1992, ApJ, 394, 228
- Breedt, E., et al., 2014, MNRAS, 443, 3174
- Carlin, J. L., et al., 2012, Research in Astronomy and Astrophysics, 12, 755
- Chen, L., et al., 2012, Research in Astronomy and Astrophysics, 12, 805
- Cojocaru, R., Torres, S., Isern, J., García-Berro, E., 2014, A&A, 566, A81
- Cui, X.-Q., et al., 2012, Research in Astronomy and Astrophysics, 12, 1197
- De Gennaro, S., von Hippel, T., Winget, D. E., Kepler, S. O., Nitta, A., Koester, D., Althaus, L., 2008, AJ, 135, 1
- Debes, J. H., Hoard, D. W., Wachter, S., Leisawitz, D. T., Cohen, M., 2011, ApJS, 197, 38
- Deng, L.-C., et al., 2012, Research in Astronomy and Astrophysics, 12, 735
- Drake, A. J., et al., 2009, ApJ, 696, 870
- Drake, A. J., et al., 2014, MNRAS, 441, 1186
- Dufour, P., Kilic, M., Fontaine, G., Bergeron, P., Lachapelle, F., Kleinman, S. J., Leggett, S. K., 2010, ApJ, 719, 803
- Dufour, P., et al., 2007, ApJ, 663, 1291
- Falcon, R. E., Winget, D. E., Montgomery, M. H., Williams, K. A., 2010, ApJ, 712, 585
- Farihi, J., Becklin, E. E., Zuckerman, B., 2005, ApJS, 161, 394
- Farihi, J., Jura, M., Zuckerman, B., 2009, ApJ, 694, 805
- Gänsicke, B. T., Marsh, T. R., Southworth, J., Rebassa-Mansergas, A., 2006, Science, 314, 1908



**Table 4.** Format of the catalogue of LAMOST white dwarfs. The full catalogue can be accessed online via the VizieR catalogue access tool.

Column No.	Heading	Description
1	sdss name	SDSS objects name (SDSS + J2000 coordinates)
2	ra	right ascension
3	dec	declination
4	probability	The <i>probability of being a WD</i> computed for this object in Gentile Fusillo et al. (2015)
5	umag	SDSS <i>u</i> band PSF magnitude
6	umag err	SDSS <i>u</i> band PSF magnitude uncertainty
7	gmag	SDSS <i>g</i> band PSF magnitude
8	gmag err	SDSS <i>g</i> band PSF magnitude uncertainty
9	rmag	SDSS <i>r</i> band PSF magnitude
10	rmag err	SDSS <i>r</i> band PSF magnitude uncertainty
11	imag	SDSS <i>i</i> band PSF magnitude
12	imag err	SDSS <i>i</i> band PSF magnitude uncertainty
13	zmag	SDSS <i>z</i> band PSF magnitude
14	zmag err	SDSS <i>z</i> band PSF magnitude uncertainty
15	ppmra	proper motion in right ascension (mas/yr)
16	ppmra err	proper motion in right ascension uncertainty (mas/yr)
17	ppmdec	proper motion in right declination (mas/yr)
18	ppmdec err	proper motion in right declination uncertainty (mas/yr)
19	Simbad classification	Currently available Simbad classifications
20	LAMOST spec ID	Unique spectra identifier composed of MJD (modified Julian date) of the observation, plate ID, spectrograph ID and a fiber ID
21	LAMOST class	classification of the object based on our visual inspection of its LAMOST spectra
22	$T_{\text{eff}}$	effective temperature calculated for DA white dwarfs (sect. 6)
23	$T_{\text{eff}}$ err	uncertainty in the effective temperature calculated for DA white dwarfs (sect. 6)
24	$\log g$	surface gravity calculated for DA white dwarfs (sect. 6)
25	$\log g$ err	uncertainty in the surface gravity calculated for DA white dwarfs (sect. 6)
26	$M/M_{\odot}$	mass of the white dwarfs calculated for DA white dwarfs (sect. 6)
27	$M/M_{\odot}$ err	uncertainty in mass the of the white dwarfs calculated for DA white dwarfs (sect. 6)

Gänsicke, B. T., Koester, D., Girven, J., Marsh, T. R., Steeghs, D., 2010, *Science*, 327, 188  
Gentile Fusillo, N. P., Gnsicke, B. T., Greiss, S., 2015, *MNRAS*, 448, 2260  
Giammichele, N., Bergeron, P., Dufour, P., 2012, *ApJS*, 199, 29  
Girven, J., Gänsicke, B. T., Steeghs, D., Koester, D., 2011, *MNRAS*, 417, 1210  
Holberg, J. B., Bergeron, P., 2006, *AJ*, 132, 1221  
Hu, Q., Wu, C., Wu, X.-B., 2007, *A&A*, 466, 627  
Iben, I. J., Ritossa, C., Garcia-Berro, E., 1997, *ApJ*, 489, 772  
Kepler, S. O., Kleinman, S. J., Nitta, A., Koester, D., Castanheira, B. G., Giovannini, O., Costa, A. F. M., Althaus, L., 2007, *MNRAS*, 375, 1315  
Kepler, S. O., et al., 2015, *MNRAS*, 446, 4078  
Kilic, M., Brown, W. R., Allende Prieto, C., Kenyon, S. J., Heinke, C. O., Agüeros, M. A., Kleinman, S. J., 2012, *ApJ*, 751, 141  
Kleinman, S. J., et al., 2013, *ApJS*, 204, 5  
Koester, D., 2010, *Memorie della Societa Astronomica Italiana*, 81, 921  
Koester, D., Kepler, S. O., Kleinman, S. J., Nitta, A., 2009, *Journal of Physics Conference Series*, 172, 012006  
Koester, D., Gänsicke, B. T., Farihi, J., 2014, *A&A*, 566, A34  
Liebert, J., Bergeron, P., Holberg, J. B., 2005, *ApJS*, 156, 47  
Limoges, M.-M., Bergeron, P., 2010, *ApJ*, 714, 1037

Liu, X.-W., et al., 2014, in Feltzing, S., Zhao, G., Walton, N. A., Whitelock, P., eds., *IAU Symposium*, vol. 298 of *IAU Symposium*, p. 310  
Luo, A.-L., et al., 2015, *ArXiv e-prints*  
Martin, D. C., et al., 2005, *ApJ Lett.*, 619, L1  
McCook, G. P., Sion, E. M., 1999, *ApJS*, 121, 1  
Morgan, J. S., Burgett, W., Onaka, P., 2014, in *Society of Photo-Optical Instrumentation Engineers (SPIE) Conference Series*, vol. 9145, p. 0  
Morrissey, P., et al., 2005, *ApJ Lett.*, 619, L7  
Oswalt, T. D., Smith, J. A., Wood, M. A., Hintzen, P., 1996, *Nat*, 382, 692  
Rebassa-Mansergas, A., Gänsicke, B. T., Rodríguez-Gil, P., Schreiber, M. R., Koester, D., 2007, *MNRAS*, 382, 1377  
Rebassa-Mansergas, A., Gänsicke, B. T., Schreiber, M. R., Koester, D., Rodríguez-Gil, P., 2010, *MNRAS*, 402, 620  
Rebassa-Mansergas, A., Nebot Gomez-Moran, A., Schreiber, M., Girven, J., Gänsicke, B., 2011, *MNRAS*, 413, 1121  
Rebassa-Mansergas, A., et al., 2015, *ArXiv e-prints*  
Ren, J. J., et al., 2014, *A&A*, 570, A107  
Renedo, I., Althaus, L. G., Miller Bertolami, M. M., Romero, A. D., Córscico, A. H., Rohrmann, R. D., García-Berro, E., 2010, *ApJ*, 717, 183  
Schmidt, G. D., Liebert, J., Harris, H. C., Dahn, C. C., Leggett, S. K., 1999, *ApJ*, 512, 916  
Sion, E. M., Leckenby, H. J., Szkody, P., 1990, *ApJ Lett.*, 364, L41  
Sion, E. M., Holberg, J. B., Oswalt, T. D., McCook, G. P.,

- Wasatonic, R., Myszka, J., 2014, *AJ*, 147, 129
- Smartt, S. J., Eldridge, J. J., Crockett, R. M., Maund, J. R., 2009, *MNRAS*, 395, 1409
- Song, Y.-H., et al., 2012, *Research in Astronomy and Astrophysics*, 12, 453
- Steele, P. R., et al., 2013, *MNRAS*, 429, 3492
- Torres, S., García-Berro, E., Krzesinski, J., Kleinman, S. J., 2014, *A&A*, 563, A47
- Tremblay, P.-E., Ludwig, H.-G., Steffen, M., Bergeron, P., Freytag, B., 2011, *A&A*, 531, L19
- Tremblay, P.-E., Ludwig, H.-G., Steffen, M., Freytag, B., 2013, *A&A*, 559, A104
- Verbeek, K., et al., 2013, *MNRAS*, 434, 2727
- Wilson, D. J., Gänsicke, B. T., Koester, D., Raddi, R., Breedt, E., Southworth, J., Parsons, S. G., 2014, *MNRAS*, 445, 1878
- Yuan, H.-B., et al., 2015, *MNRAS*, 448, 855
- Zhang, Y.-Y., et al., 2013, *AJ*, 146, 34
- Zhao, G., Zhao, Y.-H., Chu, Y.-Q., Jing, Y.-P., Deng, L.-C., 2012, *Research in Astronomy and Astrophysics*, 12, 723
- Zhao, J. K., Luo, A. L., Oswalt, T. D., Zhao, G., 2013, *AJ*, 145, 169
- Zuckerman, B., Reid, I. N., 1998, *ApJ Lett.*, 505, L143